Available online at www.sciencedirect.com
ScienceDirect
Optical Materials xxx (2007) xxx–xxx
OPTICAL Materials
www.elsevier.com/locate/optmat

Structure and photoluminescence of Nd:Y_2O_3 grown by molecular beam epitaxy

I.C. Robin [a,*], R. Kumaran [a], S. Penson [a], S.E. Webster [a], T. Tiedje [a,1], A. Oleinik [b]

[a] *Advanced Materials and Process Engineering Laboratory, Department of Physics and Astronomy, University of British Columbia, Vancouver, Canada BC V6T 1Z4*

[b] *Zecotek Medical Systems Singapore Pte. Ltd., 20, Science Park Road, #01-23/25, TeleTech Park, Science Park II, Singapore 117674*

Received 18 October 2006; received in revised form 5 January 2007; accepted 1 March 2007

Abstract

Crystalline yttrium oxide films have been grown on Si (0 0 1) and sapphire (0001) substrates by molecular beam epitaxy using molecular oxygen and thermal evaporation of yttrium. Neodymium doped films showed strong room temperature photoluminescence from the rare earth ions. The dependence of luminescence intensity on neodymium concentration was studied and a maximum was estimated to occur at 2 at.% assuming complete neodymium incorporation. The structural properties of the films were characterized using X-ray diffraction.

© 2007 Elsevier B.V. All rights reserved.

PACS: 42.55.Rz; 81.15.−z

Keywords: Oxide thin films; Rare-earth doped oxides; Planar waveguides

1. Introduction

Solid state lasers in the form of planar waveguides have several advantages over conventional bulk designs. Planar waveguide lasers (PWL) offer better overlap between the output laser light and the pump beam within the active layer, and the geometry allows for more efficient heat removal because of a higher surface-area to volume ratio. PWLs have been fabricated by several methods, including liquid phase epitaxy [1] and pulsed laser deposition [2]. PWLs grown by molecular beam epitaxy (MBE) should yield lower densities of thermodynamic defects due to lower growth temperatures compared with bulk crystals grown from a melt. In addition MBE presents a convenient way of controlling the distribution of rare earth dopants simply by changing the flux during growth.

Yttrium oxide (Y_2O_3) has previously been investigated as an active host material for lanthanide ions [3]. Its refractory nature and optical clarity over a wide spectral region make it attractive as a laser host. The thermal conductivity of Y_2O_3 is approximately twice as large as that of yttrium aluminum garnet (YAG), and the thermal expansion coefficient is similar [4]. It is difficult to grow large high-quality Y_2O_3 single crystals by conventional methods because of the high melting temperature (≈2430 °C) of Y_2O_3 and structural phase transitions at ≈2280 °C. Instead, Lu et al. have synthesized Nd^{3+}:Y_2O_3 in ceramic form [5]. Alternatively these difficulties can be overcome by use of MBE, which can be carried out at temperatures well below the melting point.

Y_2O_3 has been grown on silicon substrates using different approaches such as ion cluster beam [6] and electron beam evaporation [7–9]. In the previous work, the motivation was to use Y_2O_3 as a dielectric in silicon integrated

* Corresponding author.
E-mail addresses: icrobin@hotmail.com (I.C. Robin), raveen@phas.ubc.ca (R. Kumaran).
[1] Also at Department of Electrical and Computer Engineering, University of British Columbia

0925-3467/$ - see front matter © 2007 Elsevier B.V. All rights reserved.
doi:10.1016/j.optmat.2007.03.003

circuits since it has a high permittivity ($\kappa = 18$). The growth of Y_2O_3 on silicon substrates is also interesting for the fabrication of PWLs because it offers the possibility of integration into silicon chips. In this paper we describe MBE growth of Y_2O_3 on Si (001) and sapphire (0001) substrates. Sapphire substrates are useful for PWLs because their low refractive index ($n_{Al_2O_3} \approx 1.77$ and $n_{Y_2O_3} \approx 1.85$ at 1 μm) facilitates the creation of waveguides.

2. Experimental

To grow Y_2O_3, we used an yttrium metal effusion cell heated between 1600 °C and 1750 °C to obtain yttrium fluxes between 5×10^{-8} and 5×10^{-7} Torr, measured with an ion gauge placed in front of the substrate. Oxygen is introduced into the chamber through a leak valve, and the oxygen flux is inferred from the background pressure in the growth chamber. The oxygen partial pressure during Y_2O_3 growth is chosen to be typically equal to ten times the yttrium flux. The Y_2O_3 growth rate as measured with a quartz crystal is typically between 100 and 800 nm/h. To dope the Y_2O_3, a neodymium cell heated to about 1000 °C is used to obtain a neodymium flux of a few percent of the yttrium flux. Growth temperatures of up to 1100 °C were investigated. The growth temperature was controlled by a thermocouple and checked with a pyrometer. We studied the influence of the growth temperature, the oxygen/yttrium flux ratio and Y/Nd flux ratio on the structural and photoluminescence (PL) properties of the neodymium doped samples.

For the growths on silicon substrates, the substrates were HF deoxidized in a clean environment before being introduced into the growth chamber and heated to 900 °C to obtain a clean Si surface free of oxide. We deposited about 1 nm of yttrium metal before the growth of Y_2O_3 to avoid the reoxidation of the HF cleaned substrate and the formation of a SiO_2 interfacial layer. After the initial Y layer, the yttrium cell was closed and a partial oxygen pressure typically around 2.5×10^{-6} Torr was introduced in the growth chamber. The Y_2O_3 growth was started by reopening the yttrium cell shutter when the pressure in the growth chamber was stabilized.

For the growths on sapphire substrates, pre-treatment involved metallizing the back surfaces with chromium and molybdenum to improve heater radiation absorption followed by cleaning with hot acetone and methanol. The growth of Y_2O_3 was started by opening the yttrium cell shutter once a partial oxygen pressure around 2.5×10^{-6} Torr had been established.

3. Results and discussion

For growths on Si (001), single crystal orientation along the growth axis of Y_2O_3 was found for growth temperatures between 350 and 800 °C. For a growth temperature of 350 °C the heteroepitaxial relation Y_2O_3 (111) ‖ Si (001) is dominant. For a growth temperature of 650 °C, Y_2O_3 (001) ‖ Si (001) is the dominant growth mode. Fig. 1a presents the X-ray diffraction (XRD) pattern of a 60 nm thick Y_2O_3 sample grown at 800 °C. It shows the Y_2O_3 (110) ‖ Si (001) heteroepitaxial relation: the two strong peaks correspond to Y_2O_3 (440) and (880). This growth temperature gives the best structural quality in terms of the width of the Y_2O_3 peaks in rocking curve measurements. In the inset of Fig. 1a, we show the rocking curve on the (440) peak of the same sample. The width of 1.7 degrees is one of the best values reported in the literature [8,9]. For a growth temperature of 1000 °C the XRD pattern does not contain any Y_2O_3 peaks but only YSi_2 peaks. Those peaks were also observed at lower temperature, when an oxygen/yttrium flux ratio smaller than 10 was used at growth temperatures between 350 and 800 °C. They were also observed by Dimoulas et al. for a sample grown at 610 °C [7]. In our case, the growth of a thin yttrium metal layer before the Y_2O_3 growth seems to avoid the formation of YSi_2 up to a growth temperature of 800 °C. However, Cho et al. [6] also observed YSi_2 peaks when starting the growth with yttrium metal at 700 °C. In

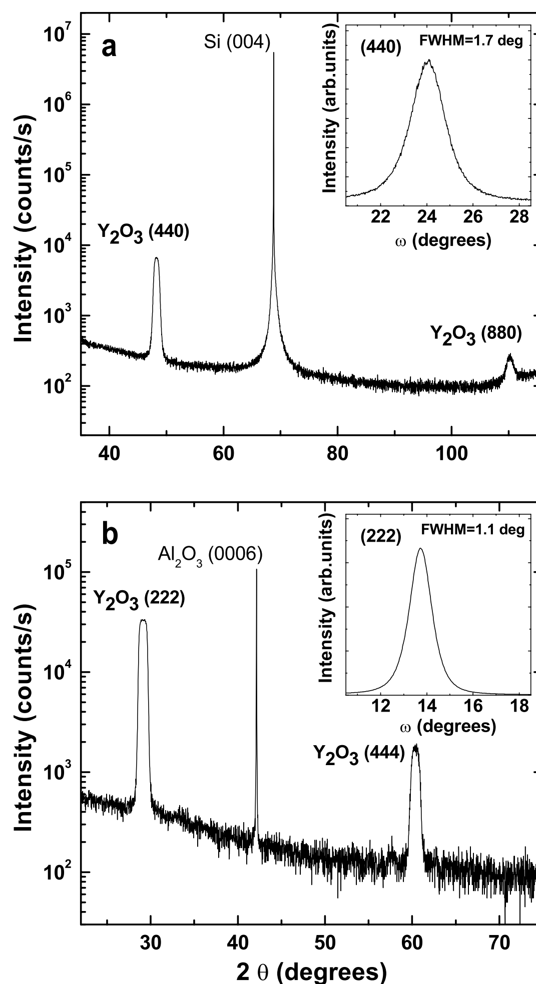

Fig. 1. XRD $\theta/2\theta$ scans for Y_2O_3 films grown (a) on a Si (001) substrate and (b) on a sapphire (0001) substrate. The insets show omega scans of the (440) peak for the sample grown on silicon and the (222) peak of the sample grown on sapphire.

our growth procedure, we expose the thin yttrium metal layer to oxygen before starting the growth of Y_2O_3. During this step, the yttrium silicide is probably oxidized into Y_2O_3.

Fig. 1b presents the θ-2θ XRD pattern of a 1.8 μm thick Y_2O_3 sample grown on sapphire (0001) at 1100 °C. The heteroepitaxial relation found was always Y_2O_3 (1 1 1) ∥ Al_2O_3 (0001). The smallest widths of Y_2O_3 peaks in rocking curve measurements were found for growth temperatures of 1100 °C. Rocking curves on the (222) peak of Y_2O_3 exhibit widths as small as 1.1 degrees (inset of Fig. 1b, same sample).

To study the in-plane orientation, we measured X-ray diffraction from off-axis peaks of the Y_2O_3 layer and the substrate using the same samples as for Fig. 1. Fig. 2a presents a Φ scan for the (840) peak of Y_2O_3 for the sample grown on Si (0 0 1). Φ is the rotation angle around the substrate surface normal. Four peaks separated by 90° are visible on a 360° Φ range, although the (840) peak has 2-fold symmetry. The appearance of four peaks shows the existence of twin domains rotated by 90° around the Si (0 0 1) azimuth. The existence of twin domains for Y_2O_3 films grown on silicon was also found by other groups [6,7]. The Φ position of the (840) Y_2O_3 off-axis peak for one of the domains is aligned with the (311) peak of the silicon substrate within 4°. From the projection of the (840) peak on the (1 1 0) plane for the Y_2O_3 and the projection of the (311) peak on the (0 0 1) plane for the silicon we conclude that the $[1\bar{1}0]$ in-plane direction of Y_2O_3 is parallel to the [110] direction of silicon within 4°. For the other domain, the in-plane orientation is [0 0 1] Y_2O_3 ∥ [110] Si.

Fig. 2b shows a Φ scan for the (662) peak of Y_2O_3 for the sample grown on sapphire (0001). A small misalignment between the (1 1 1) direction of the Y_2O_3 and the Φ rotation axis causes a variation in relative peak intensity in Fig. 2b. Six peaks separated by 60° are visible on a 360° range although, the (662) peak has a 3-fold symmetry. This shows the existence of twin domains rotated by 60° around the sapphire (0001) azimuth. The Φ position of the (662) Y_2O_3 peak for one of the domains is aligned with the $(1 0 \bar{1} 1 0)$ peak of sapphire. From the projections of the (662) peak on the (1 1 1) plane for Y_2O_3 and of the $(1 0 \bar{1} 1 0)$ peak on the (0001) plane for sapphire we determined that the $[11\bar{2}]$ in-plane direction of Y_2O_3 is parallel to the $[10\bar{1}0]$ for sapphire. For the other domain $[11\bar{2}]$ Y_2O_3 ∥ $[1\bar{1}00]$ sapphire.

Strong PL at room temperature was measured for neodymium doped samples grown on Si (0 0 1) and on sapphire (0001). A large oxygen/yttrium flux ratio (of about 10) is a precondition for strong luminescence. Fig. 3 shows the PL in three spectral regions of a 5 μm thick Nd:Y_2O_3 sample grown on sapphire (0001) at 1100 °C. The sample had a Nd concentration estimated at 2.0 ± 0.5 at.% from the Nd/Y flux ratio. The PL excitation source is a semiconductor laser diode at 808 nm with an excitation intensity of 2 W/cm^2. Emission is analysed by a 15 cm focal length monochromator with a 600 lines/mm grating. The three spectral regions correspond to the $^4F_{3/2} \rightarrow {}^4I_{9/2}$, $^4F_{3/2} \rightarrow {}^4I_{11/2}$ and $^4F_{3/2} \rightarrow {}^4I_{13/2}$ channels of neodymium. The position of the emission lines are very similar to the ones reported for Nd:Y_2O_3 ceramic samples [5]. The strongest transitions correspond to the $^4F_{3/2} \rightarrow {}^4I_{9/2}$ channel [10].

For samples grown on silicon with an oxygen/yttrium flux ratio of 10, both neodymium emission lines and band gap emission from silicon are observed. This shows that Y_2O_3 grown in these conditions is transparent. For samples grown with an oxygen/yttrium flux ratio less than 10, the band edge emission of silicon is not visible and the PL intensity of the neodymium lines is much weaker. This shows that in this case the films are opaque which could be due to the presence of YSi_2 (YSi_2 lines are observed in the XRD spectrum when the oxygen/yttrium flux ratio is smaller than 10).

In Fig. 4, we show the dependence of integrated PL intensity of the $^4F_{3/2} \rightarrow {}^4I_{11/2}$ transitions on Nd concentration. For this study, we grew eight 430 nm thick samples of Nd:Y_2O_3 on sapphire at 1100 °C using similar growth conditions with the exception of a varying Nd/Y flux ratio.

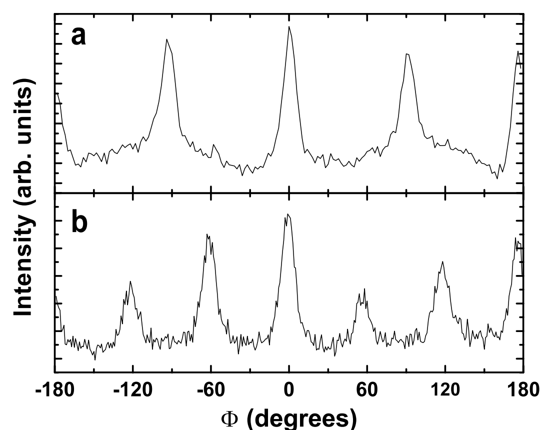

Fig. 2. Φ scans of (a) the Y_2O_3 (840) peak and (b) (662) peak for samples grown on Si (0 0 1) and sapphire (0001), respectively, showing the presence of twinning.

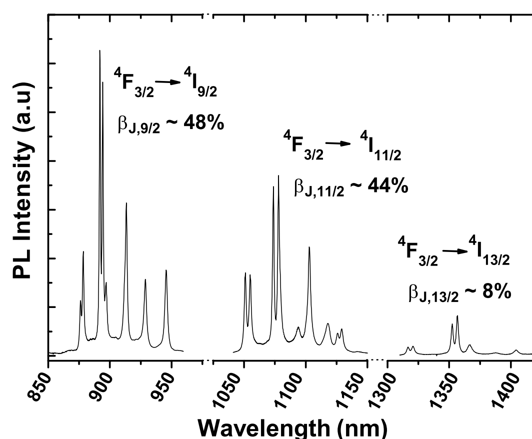

Fig. 3. PL of an approximately 2 at.% Nd:Y_2O_3 sample grown on sapphire (0001).

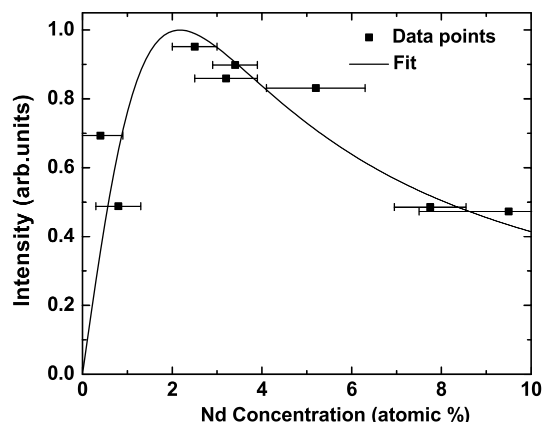

Fig. 4. PL intensity of the $^4F_{3/2} \rightarrow {}^4I_{11/2}$ transitions for varying concentrations of $Nd{:}Y_2O_3$ grown on sapphire (0001). The solid line is the expected concentration dependence for the model discussed in the text.

The Nd concentration was deduced from this flux ratio assuming complete Nd incorporation. Errors in the Nd concentration were estimated based on fluctuations in the yttrium and neodymium fluxes during growth. The error bounds were calculated from the Nd/Y flux ratio before and after growth while the average flux ratio was used to determine the Nd concentration.

At low Nd concentrations the PL intensity increases with concentration to a peak value around 2 at.%, but decreases with further increases in concentration. This quenching effect is due to cross relaxation interactions between Nd ions. Assuming an N^2 dependence on the non-radiative relaxation rate [11], we can now express the fluorescence efficiency as $1/(1 + AN^2)$ where N is the Nd concentration. Factoring in absorption, the total PL emission can be fitted to the form $BN/(1 + AN^2)$, where A and B are fitting parameters. Using this model, we find an optimal dopant concentration of 2 at.%, similar to the concentration for maximum PL intensity in Nd:YAG [12].

In conclusion, these results suggest that it will be possible to fabricate efficient $Nd{:}Y_2O_3$ planar waveguide laser structures by this method.

Acknowledgements

The authors acknowledge Zecotek Medical Systems and the Natural Sciences and Engineering Research Council of Canada for financial support.

References

[1] C.L. Bonner, C.T.A. Brown, D.P. Shepherd, W.A. Clarkson, A.C. Troper, D.C. Hanna, B. Ferrand, Opt. Lett. 23 (1998) 942.
[2] T.C. May-Smith, C. Grivas, D.P. Shepherd, R.W. Eason, M.J.F. Healy, Appl. Surf. Sci. 223 (2004) 361.
[3] A.A. Kaminskii, Phys. Stat. Sol. A 200 (2003) 215.
[4] P.H. Klein, W.J. Croft, J. Appl. Phys. 38 (1967) 1603.
[5] J. Lu, J. Lu, K. Takaichi, T. Murai, K. Takaichi, T. Uematsu, K.I. Ueda, H. Yagi, T. Yanagitani, A.A. Kaminskii, Jpn. J. Appl. Phys. 40 (2001) L1277.
[6] M.H. Cho, D.H. Ko, K. Jeong, S.W. Whangbo, C. Whang, S. Choi, S.J. Cho, J. Appl. Phys. 85 (1999) 2909.
[7] A. Dimoulas, A. Travlos, G. Vellianitis, N. Boukos, K. Argyropoulos, J. Appl. Phys. 90 (2001) 4224.
[8] G. Apostolopoulos, G. Vellianitis, A. Dimoulas, M. Alexe, R. Scholz, M. Fanciulli, D.T. Dekadjevi, C. Wiemer, Appl. Phys. Lett. 81 (2002) 3549.
[9] J. Kwo, M. Hong, A.R. Kortan, K.L. Queeney, Y.J. Chabal, J.R.L. Opila, D.A. Muller, S.N.G. Chu, B.J. Sapjeta, T.S. Lay, J.P. Mannaerts, T. Boone, H.W. Krautter, J.J. Krajewski, A.M. Sergnt, J.M. Rosamilia, J. Appl. Phys. 89 (2001) 3920.
[10] B.M. Walsh, J.M. McMahon, W.C. Edwards, N.P. Barnes, R.W. Equall, R.L. Hutcheson, J. Opt. Soc. Am. B 19 (2002) 2893.
[11] H.G. Danielmeyer, M. Blatte, P. Balmer, Appl. Phys. 1 (1973) 269.
[12] V. Lupei, A. Lupei, S. Georgescu, T. Taira, Y. Sato, I. Ikesue, Phys. Rev. B 64 (2001) 092102.

Please cite this article in press as: I.C. Robin et al., Opt. Mater. (2007), doi:10.1016/j.optmat.2007.03.003